Research Article

# Computational Analysis of Row-Column Variations in Sonic Crystals under X-Axis Lattice Constant Expansion

**Chin-to Wat[1], King-cheong Lam[2], Walter Ka-Po Lam[3], Ricky Kai-long Mak[4] and Wai-keung Anthony Loh[5]***

[1]*Division of Science, Engineering and Health Studies, School of Professional Education and Executive Development, The Hong Kong Polytechnic University, Hong Kong, China*
[2]*Division of Science, Engineering and Health Studies, School of Professional Education and Executive Development, The Hong Kong Polytechnic University, Hong Kong, China*
[3]*Division of Science, Engineering and Health Studies, School of Professional Education and Executive Development, The Hong Kong Polytechnic University, Hong Kong, China*
[4]*Department of Analytics, Operations and Systems, Kent Business School, University of Kent, Canterbury, United Kingdom*
[5]*Division of Science, Engineering and Health Studies, School of Professional Education and Executive Development, The Hong Kong Polytechnic University, Hong Kong, China*

## Abstract

This study investigates the influence of scatterer geometry, filling fraction, and array configuration on the acoustic attenuation performance of sonic crystal noise barriers (SCNBs) under plane-wave propagation. Two-dimensional acoustic simulations were conducted using COMSOL Multiphysics to evaluate elliptical and circular scatterers arranged in periodic arrays with varying row and column numbers. The lattice constants were systematically scaled to represent barrier widths ranging from 20 cm to 160 cm, resulting in corresponding changes in filling fraction. The results reveal fundamentally different acoustic behaviors between elliptical and circular geometries. Elliptical scatterers exhibit limited attenuation capability and a narrow operating window, with insertion loss (IL) generally decreasing as the number of rows increases. Column expansion yields only marginal improvements, indicating that the elongated elliptical geometry is unable to maintain coherent Bragg scattering across larger array dimensions. In contrast, circular scatterers demonstrate strong and robust attenuation over a wide range of lattice constants and filling fractions. Increasing the number of rows significantly enhances acoustic performance, with the maximum average IL increasing from 34.5 dB for the 7×3 configuration to 60.6 dB for the 11×3 configuration. Although column expansion does not produce a strictly monotonic improvement, all circular configurations maintain high attenuation levels and exhibit strong acoustic bandgap formation. Excluding an isolated anomalous peak observed in one elliptical configuration, the maximum average IL achieved by circular scatterers is more than four times greater than that of elliptical scatterers. These findings demonstrate that scatterer geometry plays a critical role in determining SCNB performance and confirm that circular scatterers offer superior acoustic attenuation, broader design flexibility, and greater potential for practical broadband noise barrier applications.

## Introduction

Rapid urbanisation and the continual growth of vehicular traffic have made environmental noise a major public health concern in modern cities. Prolonged exposure to road traffic noise can adversely affect residents living near major transportation corridors, with sleep disturbance being one of the most commonly reported impacts. Numerous epidemiological studies have demonstrated that long-term exposure to traffic noise is associated with increased risks of cardiovascular disorders, hypertension, and

SHRINE PUBLISHERS
Crafting your Achievement

**Shrine Journal of Research and Sciences (SJRS)**

**ISSN: 3069-2032**

**Volume 3 Issue 4, 2026**

**Article Information**
Received date: October 29, 2026
Published date: November 10, 2026

***Corresponding author**
Wai-keung Anthony Loh, Division of Science, Engineering and Health Studies, School of Professional Education and Executive Development, The Hong Kong Polytechnic University, Hong Kong, China

**DOI:** 10.65070/SJRS.2026.835

**Keywords**
Sonic crystal noise barrier; Insertion loss; Bragg scattering; Circular and Elliptical Scatterers; Filling fraction

**Distributed under:**
Creative Commons CC-BY 4.0

**Copyright ©** : Loh WKA

sleep-related stress and anxiety [1,2]. In Hong Kong, more than 650,000 residents are exposed to road traffic noise levels exceeding 70 dB, affecting approximately 9.2% of the population across the territory's 18 districts [3]. Given the close proximity of many residential developments to major highways and the continued increase in traffic volumes, the development and implementation of effective noise mitigation measures have become increasingly important for protecting public health and improving urban living environments.

Sonic crystals (SCs), which consist of periodic arrangements of acoustic scatterers, have emerged as a promising approach for attenuating targeted frequency ranges of environmental noise. In recent years, increasing academic and industrial attention has been directed towards the development of SC-based noise barriers. Following the pioneering work of Chong et al. [4], most studies have focused on enhancing insertion loss (IL) performance through the use of circular and C-shaped scatterers. Despite these advances, achieving effective broadband attenuation remains a major challenge. Existing studies generally report IL spectral reductions of approximately 5–7 dB at frequencies above 800–1000 Hz [5–8], which remain considerably lower than the attenuation levels of around 20 dB typically achieved by conventional solid noise barriers. Consequently, further optimisation of scatterer geometry and array configuration is required to improve the practical applicability of SC noise barriers for broadband noise mitigation.

A critical yet often overlooked consideration in the design and implementation of sonic crystal (SC) noise barriers is the limited installation space available at practical deployment sites. In Hong Kong, the minimum widths of central reserves range from approximately 1.8 m for district and local distributor roads to 2.3 m for primary distributor roads and expressways, while rural roads typically provide widths between 1.8 m and 3.3 m [9]. In practice, the effective installation width is frequently further restricted by existing road infrastructure, safety requirements, and site-specific constraints. Consequently, both the lattice constant and the maximum number of scatterer rows that can be accommodated within an SC barrier are physically constrained by the available installation space. Optimising SC configurations within these finite dimensions is therefore essential for achieving effective noise attenuation under realistic conditions. To address this practical challenge, the present study investigates the acoustic performance of circular and elliptical scatterers over the frequency range of 0–4000 Hz. Particular attention is given to evaluating the relative influence of row and column variations, as well as the effects of proportionally increasing the lattice constant in the horizontal direction, thereby providing insights into the most effective geometric configurations for space-constrained SC noise barrier applications.

## Methodology

### Computational Domain and Boundary Conditions

In this study, two-dimensional (2D) acoustic simulations were performed using the Acoustic Module in COMSOL Multiphysics®. The numerical models were designed to evaluate the acoustic attenuation of various SC configurations under plane wave excitation. The total computational domain was defined as a 340cm (width) × 60cm (height) rectangular area as shown in Figure 1, the setup mimics an anechoic chamber, featuring a central scatterer area initialized with a 20cm width, an inlet background source region of 165cm, and an outlet region of 135cm. To simulate a free-field open environment and prevent artificial boundary reflections, Perfectly Matched Layers (PMLs) were applied at both the inlet (Region S1) and outlet (Region S4) boundaries. These PMLs act as highly effective sponge layers that absorb outgoing waves, mimicking a non-reflecting infinite domain [10]. Region S2 was defined as the background pressure field, serving as the source of the incident plane wave. The SCs themselves were modeled as sound-hard boundaries (rigid bodies) with a coefficient of reflection 1. Owing to acoustic energy transmission in air which is governed by pressure gradients and restoring forces rather than discrete particle collisions, sound propagation in the absence of external energy absorbers experiences no inherent energy loss [11,12]. Consequently, the rigid SCs act as the sole impedance source in the domain, allowing the study to isolate the attenuation effects caused purely by the structure's geometry.

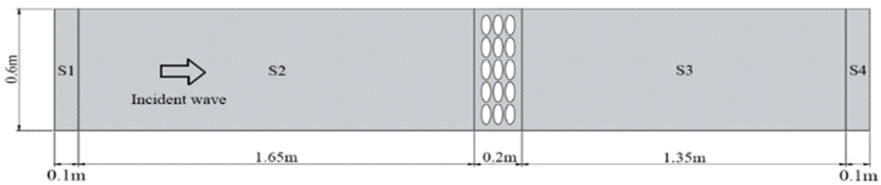



**Figure 1:** Illustration of the initial model for simulation.

**Copyright** © : Loh WKA

Figure 2 shows a planar arrangement of circular scatterers organized in a regular lattice, forming the core soniccrystal module. The number of column and row of SCs are defined along x and y axis respectively. This topview schematic illustrates the installed configuration of the scatterers within the designated central scattering zone.

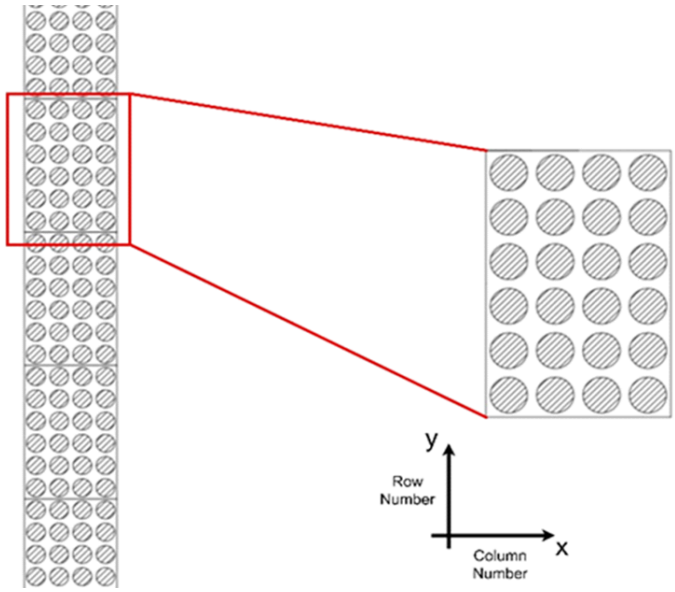



**Figure 2:** Top view of sonic crystals module installed at central scatter area.

## Scatterer Configurations and Filling Fraction

To systematically investigate the effect of structural width and lattice scaling, a total of 48 models were conducted in simulations. The central scatterer area width d was exponentially expanded from an initial 20 cm to 40 cm, 80 cm, and up to a maximum of 160 cm (which represents the maximum allowable central reserve width for rural expressways in Hong Kong). Correspondingly, the x-axis lattice constant (lx) was scaled proportionally across these domains. Filling fraction (ff) is inherently changed by varying the lattice constant. The ff for the square lattices can be expressed using equation (1):

$$ff_{square} = \frac{\pi r_0^2}{a^2} \qquad (1)$$

Elliptical scatterers with a semi-major axis to semi-minor axis ratio (a:b) of 2:1 were designed as illustrated in Figure 3. The elliptical configurations were modelled using a semi-major axis a = 22.57mm, a semi-minor axis b = 11.28mm, lattice constants $l_x$ = 40mm and $l_y$ = 54mm, and a filling fraction ff = 0.370, where $l_x$ and $l_y$ represent the lattice constants in the x and y directions, respectively. Five array configurations, namely 7×3, 9×3, 11×3, 11×2 and 11×4 (row × column), were generated, as shown in Figure 3, to investigate the effects of row and column variations on acoustic attenuation performance. For comparison, circular scatterers were modelled with a radius r = 24.43mm, lattice constants $l_x$ = $l_y$ = 50mm, and a filling fraction ff=0.75. The corresponding circular array configurations of 7×3, 9×3, 11×3, 11×2 and 11×4 are shown in Figure 4. These configurations were employed to evaluate and compare the influence of array geometry on the acoustic performance of sonic crystal noise barriers.

**Copyright** © : Loh WKA

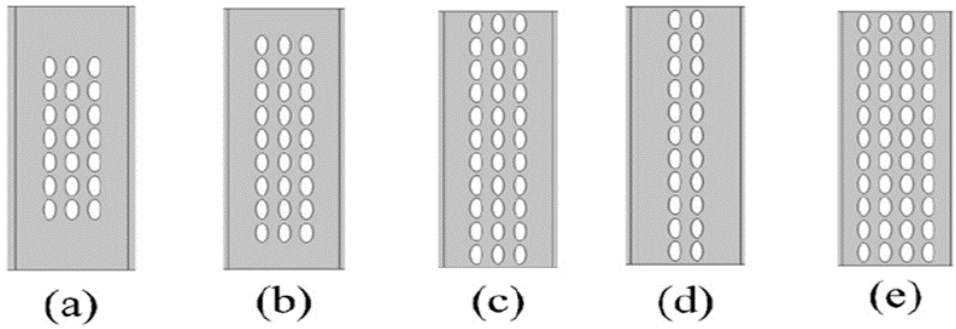



**Figure 3:** Array structure of elliptical scatterer: (a) 7×3, (b) 9×3, (c) 11×3, (d) 11×2, (e) 11×4.

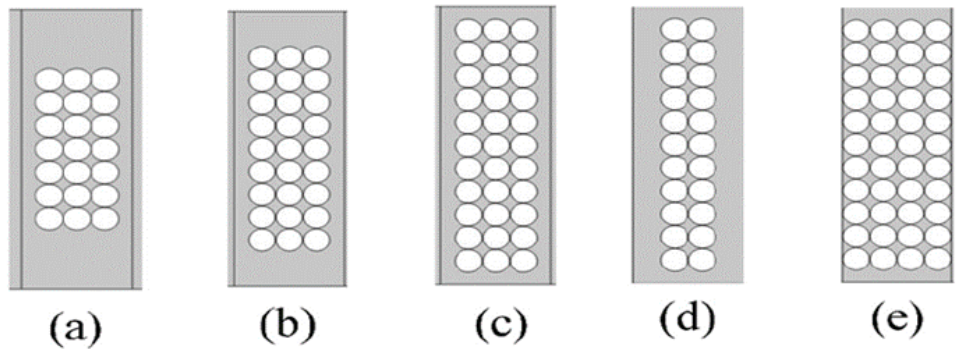



**Figure 4:** Array structure of circular scatterer: (a) 7×3, (b) 9×3, (c) 11×3, (d) 11×2, (e) 11×4.

## Insertion Loss

The performance of the SC arrays was assessed using Insertion Loss (IL), which represents the reduction of sound level in decibels (dB) when the sonic crystal noise barrier is introduced [4]. It is calculated using equation (2):

$$IL = 10log_{10}\left|\frac{P_{direct}}{P_{total,\ transmitted}}\right| \qquad (2)$$

where $P_{direct}$ and $P_{total}$ represent the acoustic power determined at the receiver without and with the sonic crystal (SC) barrier, respectively. The insertion loss (IL) quantifies the reduction in sound pressure level resulting from the introduction of the barrier between the source and the receiver, and is therefore widely adopted as a practical metric for evaluating the noise attenuation performance of SC barriers under realistic operating conditions.

Numerous studies have investigated approaches to improving the IL of SC-based noise barriers, including the incorporation of Helmholtz resonators [13]. To evaluate performance across broadband frequency spectra, the average IL is computed by converting the decibel values back to linear power ratio before averaging using equation (3):

$$IL_{average} = 10\log_{10}\left(\frac{1}{n}\sum_{i=1}^{n}10^{\frac{IL_i}{10}}\right) \qquad (3)$$

**Copyright** © : Loh WKA

## Result and Discussion

### Influences of Row Variations on Insertion Loss

The elliptical configurations with varying row numbers (7, 9, and 11 rows) as shown in Table 1 exhibit a clear decline in insertion loss (IL) as the number of rows increases, demonstrating that deeper arrays do not enhance acoustic performance for elliptical scatterers. The 7×3 arrays show the strongest sensitivity to lattice scaling, with IL rising sharply to 54.8 dB at the intermediate filling fraction (ff = 0.1851). This sharp increase may be largely attributed to the exceptionally high IL of 80.86 dB at 3021 Hz, which substantially elevates the average IL. This pronounced peak indicates that the 7row configuration achieves an optimal periodicity at moderate scatterer density, where constructive Bragg interference is maximized. However, IL collapses at both higher and lower filling fractions, falling to 5.83 dB at ff = 0.3703 and to only 3.34–4.78 dB as the lattice expands. The 9×3 arrays exhibit a more muted response, with IL increasing modestly from 4.95 dB at ff = 0.3703 to 9.04 dB at ff = 0.1851 and reaching a moderate peak of 13.9 dB at ff = 0.0926. This behaviour suggests that increasing the number of rows stabilizes scattering but simultaneously reduces the ability of the structure to generate strong bandgap attenuation. The 11×3 arrays show consistently low IL values across all filling fractions, ranging only from 2.23 dB to 2.33 dB, indicating that deeper elliptical arrays are unable to sustain coherent Bragg scattering. The elongated 2/3:1/3 aspect ratio likely contributes to phase mismatches and internal reflections that disrupt constructive interference as the array depth increases. Overall, the results demonstrate that elliptical scatterers possess a narrow geometric window for effective attenuation, with strong IL occurring only for shallow arrays at moderate filling fractions. Increasing the number of rows suppresses IL rather than enhancing it, in sharp contrast to the behaviour of circular scatterers. These findings highlight the geometric limitations of elliptical configurations and indicate that row expansion is not an effective strategy for improving SCNB performance when elliptical scatterers are used.

**Table 1:** Influence of row variations to average IL of elliptical model.

| Elliptical Model | x-axis Lattice Constant (lx /mm) | Scatterer Area Width (d / cm) | Filling Fraction (ff) | Average IL (dB) |
|---|---|---|---|---|
| 7x3 | 40 | 20 | 0.3703 | 5.83 |
| 7x3 | 80 | 40 | 0.1851 | 54.8 |
| 7x3 | 160 | 80 | 0.0926 | 3.34 |
| 7x3 | 320 | 160 | 0.0463 | 4.78 |
| 9x3 | 40 | 20 | 0.3703 | 4.95 |
| 9x3 | 80 | 40 | 0.1851 | 9.04 |
| 9x3 | 160 | 80 | 0.0926 | 13.9 |
| 9x3 | 320 | 160 | 0.0463 | 3.43 |
| 11x3 | 40 | 20 | 0.3703 | 2.24 |
| 11x3 | 80 | 40 | 0.1851 | 2.24 |
| 11x3 | 160 | 80 | 0.0926 | 2.33 |
| 11x3 | 320 | 160 | 0.0463 | 2.23 |

**Copyright** © : Loh WKA

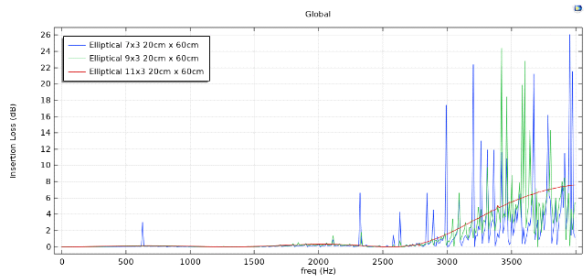
The circular configurations with varying row numbers (7, 9, and 11 rows) as shown in Table 2 exhibit a strong and generally favourable dependence of insertion loss (IL) on lattice scaling, with attenuation increasing substantially as the number of rows increases. The 7×3 arrays show a clear rise in IL as the lattice constant expands and the filling fraction decreases. IL increases from 12.1 dB at the highest density (ff = 0.7500) to 27.3 dB at ff = 0.3750, reaching a peak of 34.5 dB at ff = 0.1875. Although IL decreases to 21.2 dB at the lowest filling fraction (ff = 0.0938), the overall trend indicates that moderate geometric dilution enhances Bragg scattering for circular scatterers. The 9×3 arrays demonstrate even stronger attenuation, with IL rising to 35.9 dB at ff = 0.3750 and reaching 47.3 dB at ff = 0.0938, which is the highest IL observed for the 9row configuration. This behaviour suggests that increasing the number of rows strengthens the cumulative scattering path and improves the coherence of bandgap formation, enabling robust attenuation even at very low filling fractions. The 11×3 arrays exhibit the strongest overall IL performance among all rowvarying circular configurations. IL increases from 12.1 dB at ff = 0.7500 to 38.5 dB at ff = 0.3750, and reaches a maximum of 60.6 dB at ff = 0.1875 which is the highest IL recorded in the entire dataset. Even at the lowest filling fraction (ff = 0.0938), IL remains high at 53.1 dB, demonstrating that circular scatterers maintain phase coherence and strong Bragg interference across a wide range of geometric conditions. Unlike elliptical scatterers, where deeper arrays suppress IL, circular scatterers benefit significantly from increased row number comparing the maximum average IL (34.5 dB at 7x3 to 47.3 dB at 9x3 to 60.6 dB at 11x3), with deeper row arrays consistently producing stronger attenuation. Overall, the results show that circular scatterers possess a broad and favourable periodicity window for Bragg scattering, and that increasing the number of rows substantially enhances acoustic performance. The strong and stable IL response across all filling fractions highlights the geometric advantages of circular scatterers and confirms that row expansion is an effective strategy for improving SCNB performance in circular configurations.

**Table 2:** Influence of row variations to average IL of circular model.

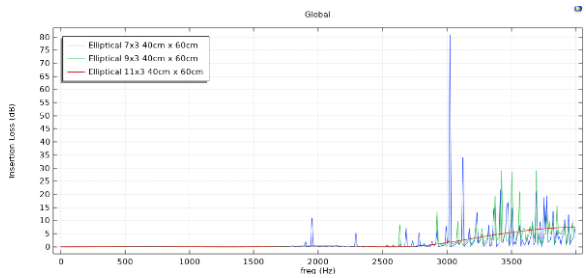
| Circular Model | x-axis Lattice Constant (lx /mm) | Scatterer Area Width (d /cm) | Filling Fraction (ff) | Average IL (dB) |
|---|---|---|---|---|
| 7x3 | 50 | 20 | 0.75 | 12.1 |
| 7x3 | 100 | 40 | 0.375 | 27.3 |
| 7x3 | 200 | 80 | 0.1875 | 34.5 |
| 7x3 | 400 | 160 | 0.0938 | 21.2 |
| 9x3 | 50 | 20 | 0.75 | 25.8 |
| 9x3 | 100 | 40 | 0.375 | 35.9 |
| 9x3 | 200 | 80 | 0.1875 | 23.2 |
| 9x3 | 400 | 160 | 0.0938 | 47.3 |
| 11x3 | 50 | 20 | 0.75 | 12.1 |
| 11x3 | 100 | 40 | 0.375 | 38.5 |
| 11x3 | 200 | 80 | 0.1875 | 60.6 |
| 11x3 | 400 | 160 | 0.0938 | 53.1 |

**Copyright** © : Loh WKA

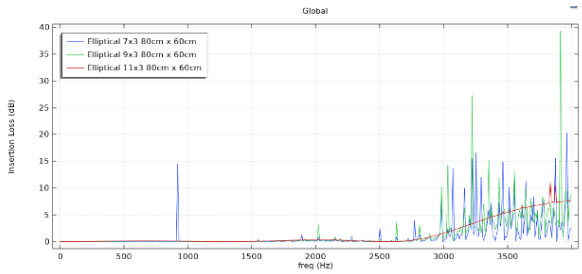
The frequency-domain results for the elliptical configurations as shown in Figure 5 reveal a consistent pattern in which the spectral insertion loss (IL) diminishes as the number of rows increases, and this behaviour persists across all scatterer area widths from 20 cm to 160 cm. For the smallest width (20 cm) in Figure 5 (a), the 7×3 array exhibits distinct IL peaks at higher frequencies, particularly above 2500 Hz, whereas the 9×3 configuration shows slightly reduced peak magnitudes and the 11×3 array remains comparatively flat with minimal attenuation across the spectrum. This trend becomes more pronounced at 40 cm in Figure 5 (b), where the 7×3 and 9×3 arrays display strong IL peaks around 3000 Hz, while the 11×3 configuration again produces only weak, nearly uniform attenuation. At 80 cm in Figure 5 (c), the spectral curves show that the 7×3 and 9×3 arrays maintain noticeable high frequency peaks, though with reduced amplitude compared with the 40 cm case, whereas the 11×3 array continues to exhibit low IL values with minimal frequency dependent variation. When the scatterer width is expanded to 160 cm in Figure 5 (d), the 7×3 and 9×3 arrays still retain moderate high frequency fluctuations, but the 11×3 configuration becomes even smoother, producing only small IL increases at higher frequencies and lacking any pronounced bandgaplike features. Across all widths, the spectral behaviour reinforces the numerical findings: elliptical scatterers generate meaningful attenuation only when the array remains shallow row arrays, and the 7×3 configuration consistently outperforms the deeper 9×3 and 11×3 arrays. The 9×3 arrays provide intermediate performance, with observable but weaker peaks, while the 11×3 arrays fail to produce strong IL at any width or frequency. Increasing scatterer width does not compensate for the loss of coherence caused by deeper row arrays; instead, the IL peaks diminish as width increases, particularly for the 7×3 and 9×3 configurations. The 11×3 arrays remain dominated by lowmagnitude, broadband IL regardless of width, indicating that the elliptical 2/3:1/3 aspect ratio does not support robust Bragg scattering when the array depth becomes large. Overall, the figures confirm that elliptical scatterers possess a narrow geometric window for effective attenuation, with strong IL occurring only for shallow row arrays and moderate widths, while deeper row arrays suppress both spectral peaks and overall attenuation.



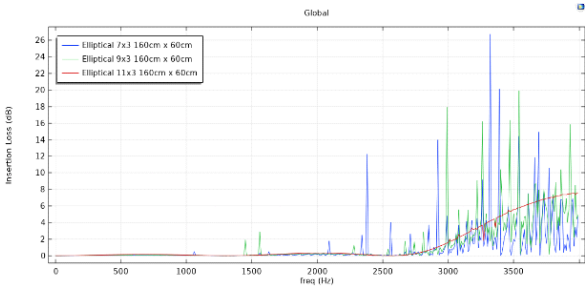

**(a)** $d$=20 cm




**(b)** $d$=40 cm




**(c)** $d$ = 80 cm

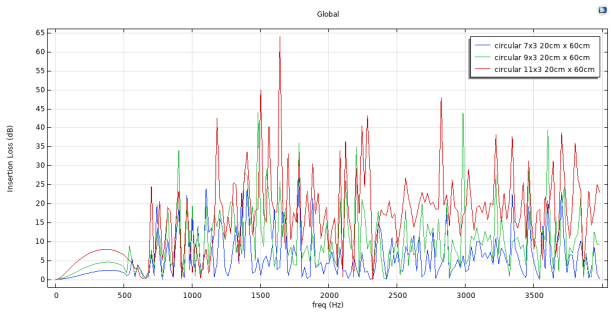



**(d)** $d$ = 160 cm

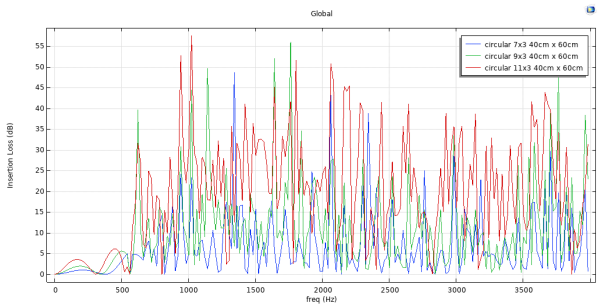
**Figure 5:** IL against frequency for row variations of elliptical model at different scatter area width $d$.

**Copyright** © : Loh WKA

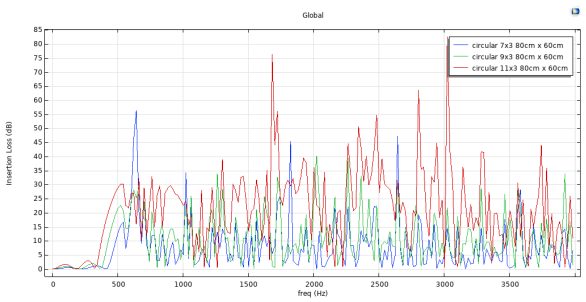
The frequency domain results for the circular configurations as shown in Figure 6 demonstrate a consistently strong and favourable dependence of insertion loss (IL) on both row number and scatterer area width, with deeper row arrays producing markedly higher attenuation across all frequencies. At the smallest width of 20 cm in Figure 6 (a), the 11×3 configuration already exhibits the highest IL, with prominent peaks distributed across the spectrum, while the 9×3 array shows intermediate performance and the 7×3 array produces comparatively lower IL. This hierarchy becomes even more pronounced at 40 cm in Figure 6 (b), where the 11×3 array displays broad, high magnitude IL peaks extending across the mid to high frequency range, whereas the 9×3 array retains strong but more localized peaks, and the 7×3 array shows moderate attenuation. At 80 cm in Figure 6 (c), the spectral curves reveal substantial amplification of IL for the 11×3 configuration, which develops dominant peaks exceeding those of both shallower arrays; the 9×3 configuration also shows strong high frequency attenuation, while the 7×3 array maintains moderate but clearly weaker IL. When the scatterer width is expanded to 160 cm in Figure 6 (d), the 11×3 array again produces the strongest IL response, with large, sustained peaks across the spectrum, while the 9×3 array shows robust but slightly lower attenuation and the 7×3 array remains the least effective. Across all widths, the circular scatterers maintain coherent Bragg scattering even at very low filling fractions, enabling strong attenuation at both mid and highfrequency ranges. Taken together, the figures confirm that circular scatterers possess a broad and stable periodicity window, where increasing the number of rows consistently strengthens IL regardless of scatterer width. Unlike the elliptical configurations, where deeper row arrays suppress attenuation, the circular arrays benefit significantly from deeper row arrays, with the 11×3 configuration outperforming the 7×3 and 9×3 arrays at every width and frequency range. Increasing scatterer width further enhances IL for deeper row arrays, producing stronger and more continuous spectral peaks. Overall, the results demonstrate that circular scatterers are highly effective for SCNB applications, with row expansion and width scaling jointly contributing to robust and frequencywide attenuation.



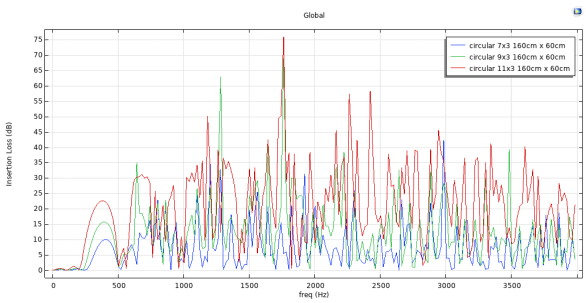

**(a)** $d$=20 cm




**(b)** $d$=40 cm




**(c)** $d$ = 80 cm




**(d)** $d$ = 160 cm

**Figure 6:** IL against frequency for row variations of circular model at different scatter area width $d$.

**Copyright** © : Loh WKA

## Influences of Column Variations on Insertion Loss

The elliptical configurations with fixed row number (11 rows) and varying column number (2, 3 and 4) as shown in Table 3 exhibit consistently low insertion loss (IL), indicating that column expansion alone does not substantially enhance the acoustic performance of elliptical scatterers. For the 11×2 arrays, IL remains below 1.1 dB across all lattice constants, ranging from 1.08 dB at the highest filling fraction (ff = 0.3703) to only 0.80–0.88 dB as the lattice expands and ff decreases. This minimal variation suggests that two-column arrays are insufficient to generate meaningful Bragg scattering, regardless of scatterer spacing. Increasing the number of columns to three produces slightly higher IL values, with attenuation rising to 2.22 dB at ff = 0.3703 and decreasing to 1.31–1.58 dB as the lattice expands. Although the IL values remain low, the modest improvement relative to the 11×2 arrays indicates that adding a third column provides a marginal increase in scattering depth, but not enough to establish a strong periodic bandgap. The 11×4 arrays show the highest IL among the column varying configurations, with attenuation increasing to 4.10 dB at ff = 0.3703 and remaining between 2.09 dB and 2.61 dB as the lattice constant increases. This pattern suggests that four columns provide a more effective scattering path length, enabling slightly stronger attenuation. However, even at four columns, IL remains far below the levels observed in the circular models or in the elliptical configurations where row number was varied. The consistently low IL across all column counts indicates that elliptical scatterers are sensitive to array geometry, and that column expansion alone does not create the conditions necessary for strong Bragg scattering. The elongated 2/3:1/3 aspect ratio limits the ability of the structure to sustain coherent attenuation. Overall, the results demonstrate that increasing the number of columns in elliptical arrays yields only marginal improvements in IL comparing the maximum average IL (1.08 dB at 11x2 to 2.22 dB at 11x3 to 4.10 dB at 11x4), with deeper column arrays consistently producing stronger attenuation. The improvement of attenuation remains weak across all filling fractions and lattice constants. These findings highlight the geometric limitations of elliptical configurations.

**Table 3:** Influence of column variations to average IL of elliptical model.

| Elliptical Model | x-axis Lattice Constant (lx /mm) | Scatterer Area Width (d /cm) | Filling Fraction (ff) | Average IL (dB) |
|---|---|---|---|---|
| 11x2 | 40 | 20 | 0.3703 | 1.08 |
| 11x2 | 80 | 40 | 0.1851 | 0.85 |
| 11x2 | 160 | 80 | 0.0926 | 0.8 |
| 11x2 | 320 | 160 | 0.0463 | 0.88 |
| 11x3 | 40 | 20 | 0.3703 | 2.22 |
| 11x3 | 80 | 40 | 0.1851 | 1.43 |
| 11x3 | 160 | 80 | 0.0926 | 1.31 |
| 11x3 | 320 | 160 | 0.0463 | 1.58 |
| 11x4 | 40 | 20 | 0.3703 | 4.1 |
| 11x4 | 80 | 40 | 0.1851 | 2.26 |
| 11x4 | 160 | 80 | 0.0926 | 2.09 |
| 11x4 | 320 | 160 | 0.0463 | 2.61 |

**Copyright** © : Loh WKA

The circular configurations with a fixed row number (11 rows) and varying column number (2, 3 and 4) as shown in Table 4 exhibit consistently strong insertion loss (IL), demonstrating that column expansion significantly enhances the acoustic performance of circular scatterers. For the 11×2 arrays, IL increases markedly as the lattice constant expands and the filling fraction decreases. At the highest density (ff = 0.7500), IL is already substantial at 26.37 dB, rising sharply to 51.2 dB at ff = 0.3750. Although IL decreases to 35.1 dB at ff = 0.1875, it increases again to 42.27 dB at the lowest filling fraction (ff = 0.0938), indicating that even sparse lattices can sustain strong Bragg scattering when circular scatterers are used. Increasing the number of columns to three further strengthens attenuation. The 11×3 arrays produce IL values of 41.44 dB at ff = 0.7500 and 38.5 dB at ff = 0.3750, followed by a dramatic increase to 60.6 dB at ff = 0.1875 which is the highest IL observed across all column varying configurations.

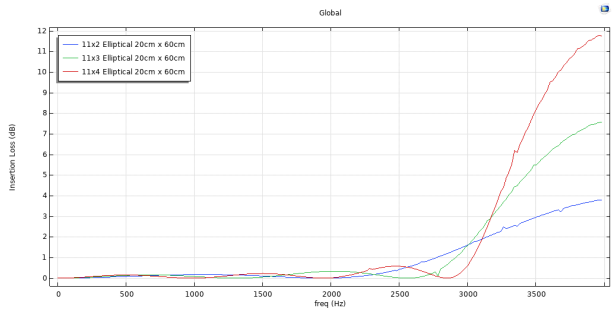
Even at the lowest filling fraction, IL remains high at 53.1 dB, demonstrating that three column circular arrays maintain phase coherence and strong bandgap formation across a wide range of geometric conditions. The 11×4 arrays exhibit the most stable and consistently high IL performance. Attenuation increases from 47.11 dB at ff = 0.7500 to 48.61 dB at ff = 0.3750, and remains strong at 52.7 dB and 56.1 dB as the lattice expands further. Unlike the elliptical configurations, where column variation produced only marginal improvements, the circular arrays show a clear and robust enhancement in IL across all column number. The circular geometry appears to support coherent scattering more effectively across multiple columns, enabling strong attenuation even under substantial lattice expansion and extremely low filling fractions. However increasing the number of column does not yield a consistent improvement in IL comparing the maximum average IL (42.27 dB at 11x2 to 60.6 dB at 11x3 to 56.1 dB at 11x4).

**Table 4:** Influence of column variations to average IL of circular model.

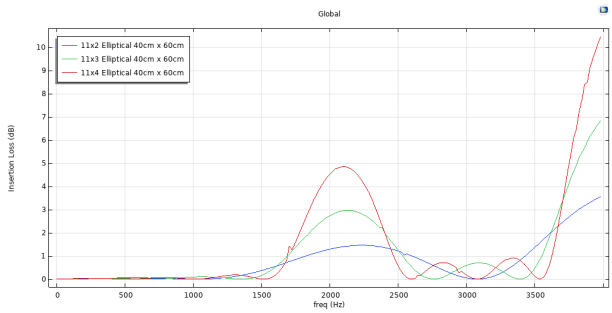
| Circular Model | x-axis Lattice Constant (lx /mm) | Scatterer Area Width (d /cm) | Filling Fraction (ff) | Average IL (dB) |
|---|---|---|---|---|
| 11x2 | 50 | 20 | 0.75 | 26.37 |
| 11x2 | 100 | 40 | 0.375 | 51.2 |
| 11x2 | 200 | 80 | 0.1875 | 35.1 |
| 11x2 | 400 | 160 | 0.0938 | 42.27 |
| 11x3 | 50 | 20 | 0.75 | 41.44 |
| 11x3 | 100 | 40 | 0.375 | 38.5 |
| 11x3 | 200 | 80 | 0.1875 | 60.6 |
| 11x3 | 400 | 160 | 0.0938 | 53.1 |
| 11x4 | 50 | 20 | 0.75 | 47.11 |
| 11x4 | 100 | 40 | 0.375 | 48.61 |
| 11x4 | 200 | 80 | 0.1875 | 52.7 |
| 11x4 | 400 | 160 | 0.0938 | 56.1 |

**Copyright** © : Loh WKA

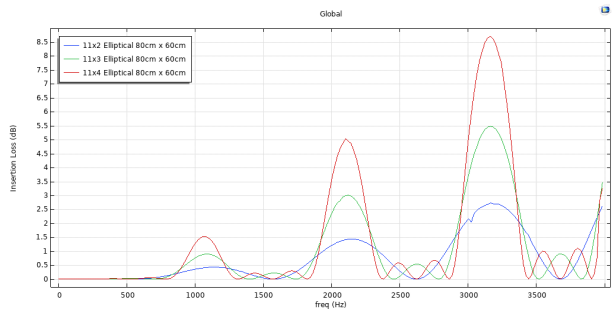
The frequency domain results for the elliptical configurations under column number variation as shown in Figure 7 reveal a consistent pattern in which increasing the number of columns enhances insertion loss (IL), although the magnitude of improvement remains modest compared with circular scatterers and is strongly constrained by the elliptical geometry. At the smallest scatterer width of 20 cm in Figure 7 (a), the 11×4 configuration exhibits the highest IL across the spectrum, with noticeable highfrequency peaks above 2500 Hz, while the 11×3 array shows intermediate attenuation and the 11×2 array remains the weakest. This hierarchy persists at 40 cm in Figure 7 (b), where the 11×4 configuration again produces the strongest IL, particularly around 2000–3500 Hz, while the 11×3 array displays moderate peaks and the 11×2 array remains comparatively flat. At 80 cm in Figure 7 (c), the spectral curves show slightly stronger high frequency peaks for the 11×4 configuration, but the overall IL remains low relative to circular models; the 11×3 and 11×2 arrays show only minor increases in IL, with limited frequency dependent structure. When the scatterer width is expanded to 160 cm in Figure 7 (d), the 11×4 configuration continues to outperform the others, producing the highest IL peaks across the spectrum, while the 11×3 array shows modest attenuation and the 11×2 array remains consistently weak. Across all widths, the IL curves for elliptical scatterers remain relatively low in magnitude, with shallow peaks and limited band gap like behaviour, indicating that column expansion alone cannot overcome the inherent limitations of the elliptical 2/3:1/3 aspect ratio. Overall, the figures confirm that elliptical scatterers exhibit only incremental improvements in IL when the number of columns is increased, and these improvements diminish as scatterer width increases. Unlike circular scatterers, which show strong and stable IL enhancement with column expansion, elliptical scatterers remain highly sensitive to geometric dilution and fail to sustain coherent Bragg scattering across deeper or wider arrays. The 11×4 configuration consistently performs best, but even its spectral peaks remain modest and narrow, while the 11×2 and 11×3 arrays produce only weak attenuation across all widths. These results reinforce the conclusion that elliptical scatterers possess a narrow and fragile periodicity window, and that column expansion is not an effective strategy for achieving strong SCNB performance when elliptical geometries are used.



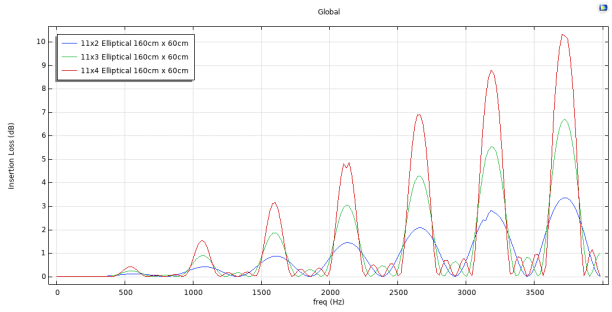

**(a)** $d$=20 cm




**(b)** $d$=40 cm




**(c)** $d$ = 80 cm

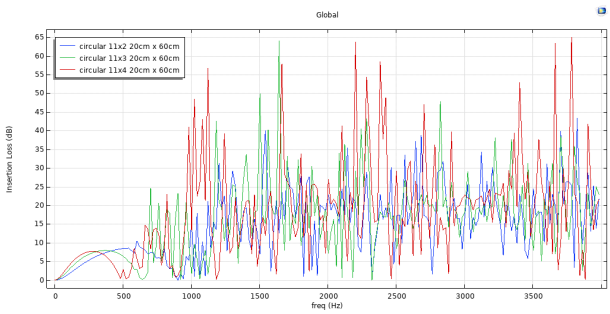



**(d)** $d$ = 160 cm

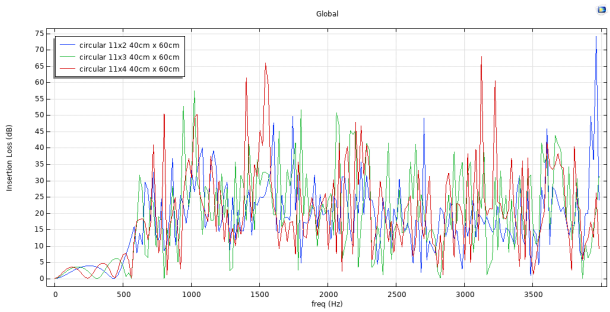
**Figure 7:** IL against frequency for column variations of elliptical model at different scatter area width $d$.

**Copyright** © : Loh WKA

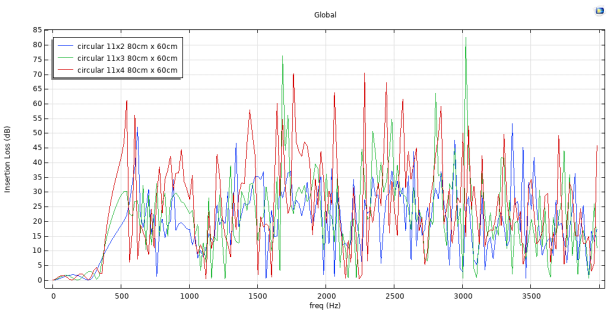
The frequency domain results for the circular configurations under column number variation as shown in Figure 8 demonstrate a clear and robust enhancement in insertion loss (IL) as the number of columns increases, and this behaviour is consistently observed across all scatterer area widths from 20 cm to 160 cm. At the smallest width of 20 cm in Figure 8 (a), the 11×4 configuration already produces the strongest IL response, with pronounced peaks distributed across the mid and highfrequency ranges, while the 11×3 array shows intermediate attenuation and the 11×2 array remains comparatively weak. This hierarchy becomes more pronounced at 40 cm in Figure 8 (b), where the 11×4 configuration exhibits broad, high magnitude IL peaks exceeding 60 dB, particularly above 2000 Hz, whereas the 11×3 array retains strong but slightly lower peaks and the 11×2 array shows moderate attenuation. At 80 cm in Figure 8 (c), the spectral curves reveal further amplification of IL for the 11×4 configuration, which develops dominant peaks across the spectrum, while the 11×3 array continues to show strong attenuation and the 11×2 array remains the least effective. When the scatterer width is expanded to 160 cm in Figure 8 (d), the 11×4 configuration again produces the highest IL values, with large, sustained peaks across the entire frequency range, while the 11×3 array shows robust but slightly lower attenuation and the 11×2 array maintains moderate IL. Across all widths, the circular scatterers maintain coherent Bragg scattering even at very low filling fractions, enabling strong attenuation at both mid and highfrequency ranges. Overall, the figures confirm that circular scatterers possess a broad and stable periodicity window, where increasing the number of columns consistently strengthens IL regardless of scatterer width. Unlike elliptical scatterers, which show only modest improvements with column expansion, the circular arrays benefit significantly from additional columns, with the 11×4 configuration outperforming the 11×2 and 11×3 arrays at every width and frequency range. Increasing scatterer width further enhances IL for deeper column configurations, producing stronger and more continuous spectral peaks.



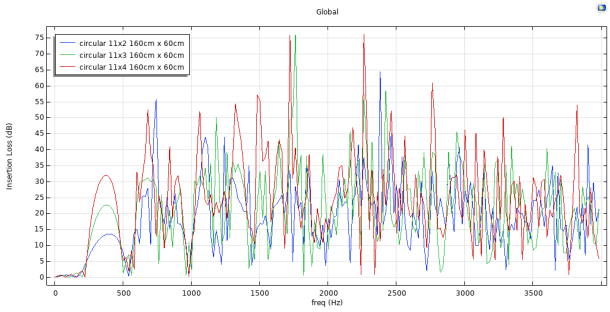

**(a)** $d$=20 cm




**(b)** $d$=40 cm




**(c)** $d$ = 80 cm




**(d)** $d$ = 160 cm

**Figure 8:** IL against frequency for column variations of circular model at different scatter area width $d$.

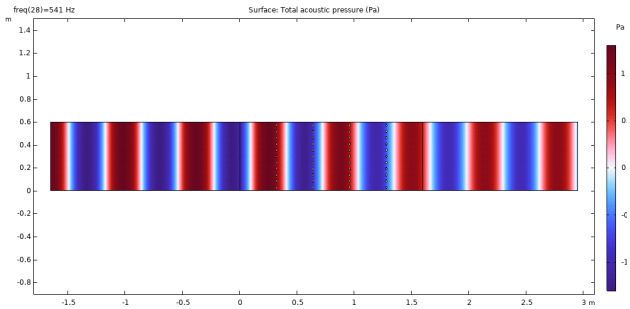
**Copyright** © : Loh WKA

## Comparison of the Influences on Rows and Columns

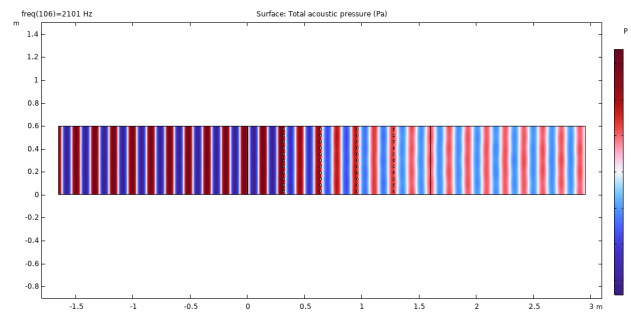
A clear contrast emerges between row and column variations when comparing the acoustic behaviour of elliptical and circular scatterers. For elliptical configurations, changes in the number of rows exert a much stronger influence on insertion loss (IL) than changes in the number of columns. Increasing the number of rows consistently suppresses IL, with deeper arrays unable to maintain coherent Bragg scattering. Shallow arrays with moderate filling fractions produce the only meaningful attenuation, while deeper arrays rapidly lose phase coherence and generate only weak, broadband IL. Column variation, in contrast, produces only minor improvements. Even when the number of columns is increased to four, IL remains low, and the overall spectral response shows only shallow peaks. This behaviour indicates that elliptical scatterers are highly sensitive to array depth but largely insensitive to lateral expansion, with their elongated geometry limiting the ability to sustain significant improvement across columns. Circular scatterers exhibit the opposite trend. Row expansion significantly enhance IL, and deeper or wider arrays consistently produce stronger attenuation across all scatterer widths. Increasing the number of rows strengthens the cumulative scattering path, enabling robust bandgap formation even at very low filling fractions across the mid and high frequency ranges. Circular scatterers maintain phase coherence across both deep row arrays and large scatterer width, demonstrating a wide geometric tolerance that supports strong Bragg scattering under a broad range of lattice constants. However, the effect of column variation in circular scatterers is not governed by a simple monotonic relationship. Overall, the results indicate that elliptical scatterers are row limited, with acoustic performance deteriorating as the number of rows increases, whereas circular scatterers are rowenhanced, benefiting significantly from greater array depth. Excluding the anomalously high IL value of 54.8 dB observed for the 7×3 elliptical configuration at a filling fraction of 0.1851, the maximum average IL achieved by the elliptical arrays is only 13.9 dB. In contrast, the circular arrays attain a maximum average IL of 60.6 dB, which is more than four times higher than the corresponding elliptical value. This substantial difference demonstrates that circular scatterers are considerably more effective at sustaining coherent Bragg scattering and forming strong acoustic bandgaps over a wide range of geometric configurations. The superior attenuation performance of the circular geometry highlights its clear advantage for sonic crystal noise barrier (SCNB) applications, particularly where strong and broadband noise reduction is required.

## Comparison of the Acoustic Pressure Pattern

The acoustic pressure pattern at different IL can be observed in Figure 9 for a representative model of elliptical scatterer with 11x4 at d = 160 cm. At 541 Hz as shown in Figure 9 (a), the insertion loss is only 0.42 dB, which indicates that the central sonic-crystal array provides little attenuation at this frequency. This agrees well with the acoustic-pressure distribution in the figure. Before reaching the central barrier, the sound field contains strong alternating red and blue bands. After passing through the sonic crystals, similarly strong and well-defined red and blue bands are still present over most of the downstream region. At 2101 Hz as shown in Figure 9 (b), the IL increases to 4.81 dB. Correspondingly, some weakening of the acoustic-pressure field can be observed after the sound wave passes through the central sonic crystals. The upstream region displays strongly saturated red and blue bands, whereas the downstream bands are generally less pronounced. The most significant change occurs at 3701 Hz as shown in Figure 9 (c), where the IL reaches 10.33 dB. The downstream region shows a large portion of the field approaching white or very light red/blue colour. Taken together, the figures indicate a strong frequency dependence of the acoustic performance of the central sonic-crystal noise barrier. The numerical IL values therefore agree qualitatively with the simulated acoustic-pressure distributions: increasing IL from 0.42 to 4.81 and then 10.33 dB is accompanied by a progressively stronger reduction in the amplitude of the pressure field behind the sonic-crystal barrier.

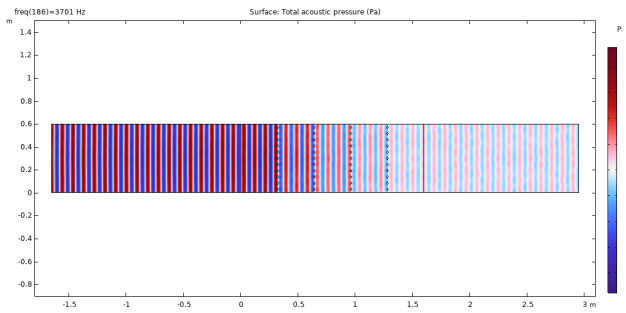



**(a)** Frequency at 541Hz (IL = 0.42)




**(b)** Frequency at 2101Hz (IL = 4.81)

**Copyright** © : Loh WKA




**(c)** Frequency at 3701Hz (IL = 10.33)

**Figure 9:** Acoustic pressure pattern of 11×4 at d = 160 cm of elliptical model at different frequencies. (a) Frequency at 541Hz; (b) Frequency at 2101Hz; (c) Frequency at 3701Hz.

## Conclusion

This study systematically investigated the acoustic attenuation performance of sonic crystal (SC) noise barriers by analyzing the effects of row and column variations under x-axis lattice constant expansion across a frequency spectrum from 0 to 4000Hz. The results demonstrate that the acoustic performance of sonic crystal noise barriers is strongly dependent on scatterer geometry, filling fraction, and array configuration. A fundamental distinction was observed between elliptical and circular scatterers in their ability to sustain Bragg scattering and generate effective acoustic attenuation. Although both geometries exhibited sensitivity to lattice scaling and filling fraction, their responses to variations in row and column numbers were markedly different.

For elliptical scatterers, increasing the number of rows consistently reduced insertion loss, indicating that deeper arrays do not favour coherent wave interference. Except for the isolated 7×3 configuration at a filling fraction of 0.1851, which was dominated by a single exceptionally high spectral peak, attenuation remained relatively low across all array configurations. The maximum average IL obtained from the non-anomalous elliptical cases was only 13.9 dB. Similarly, increasing the number of columns produced only marginal improvements, with the highest average IL increasing from 1.08 dB for the 11×2 array to 4.10 dB for the 11×4 array. These findings suggest that the elongated 2/3:1/3 elliptical geometry is unable to maintain phase coherence over larger array dimensions, resulting in weak and unstable bandgap formation. Consequently, elliptical scatterers possess only a narrow geometric window in which meaningful attenuation can be achieved.

In contrast, circular scatterers demonstrated strong and robust acoustic performance across a broad range of lattice constants and filling fractions. Row expansion was found to be particularly effective, with the maximum average IL increasing from 34.5 dB for the 7×3 configuration to 47.3 dB for the 9×3 configuration and reaching 60.6 dB for the 11×3 configuration. This behaviour indicates that deeper circular arrays enhance the cumulative scattering path and promote coherent Bragg interference, resulting in stronger bandgap formation and higher attenuation. Column variation also produced substantial IL values, with all configurations exhibiting attenuation exceeding 26 dB and peak performance occurring in the 11×3 array. However, the influence of column number was not monotonic, indicating that optimal attenuation is governed by the interaction between periodicity, filling fraction, and wave interference rather than by column count alone.

A direct comparison between the two geometries highlights the clear superiority of circular scatterers. Excluding the anomalous elliptical result, the highest average IL achieved by the circular configurations (60.6 dB) was more than four times greater than that of the elliptical configurations (13.9 dB). Furthermore, circular scatterers maintained strong attenuation over a much wider range of geometric conditions, demonstrating greater tolerance to changes in lattice scaling, filling fraction, and array dimensions. These results indicate that circular scatterers are considerably more effective at sustaining coherent Bragg scattering and generating strong acoustic bandgaps.

## Acknowledgment

This research is inspiring by the research study on “Exploring the Use of Sonic Crystal in Noise Barriers” (UGC/FDS24/E12/23). The authors would like to thank Professor Chak-yin Tang and Research Centre for Green Energy, Transport and Building (RCGETB) for providing access to the commercial COMSOL Multiphysics computational resources used in this study.

## Funding

This work was fully supported by a grant from the Research Grants Council of the Hong Kong Special Administrative Region, China (RGC Project Ref. No. UGC/FDS24/E12/23).

**Copyright** © : Loh WKA

## References

1. De Kluizenaar Y, Janssen SA, van Lenthe FJ, Miedema HME, Mackenbach JP (2009) Long-Term Road Traffic Noise Exposure Is Associated with an Increase in Morning Tiredness. J Acoust Soc Am 126(2): 626-633.

2. Babisch W, Beule B, Schust M, Kersten N, Ising H (2005) Traffic Noise and Risk of Myocardial Infarction. Epidemiology 16(1): 33-40.

3. E. P. Department "Noise." Enviromental Protection Department.

4. Chong YB (2012) Sonic Crystal Noise Barriers.

5. Sutherland LC, Daigle GA (1997) Atmospheric Sound Propagation. In: Encyclopedia of Acoustics; John Wiley & Sons, Ltd. pp. 341-365.

6. D'Orazio T, Asdrubali F, Godinho L, Veloso M, Mendes PA (2023) Experimental and Numerical Analysis of Wooden Sonic Crystals Applied as Noise Barriers. Environments 10(7): 116.

7. Morandi F, Miniaci M, Marzani A, Barbaresi L, Garai M (2016) Standardised Acoustic Characterisation of Sonic Crystals Noise Barriers: Sound Insulation and Reflection Properties. Applied Acoustics 114: 294-306.

8. Koussa F, Defrance J, Jean P, Benon BP (2012) Transport Noise Reduction by Low Height Sonic Crystal Noise Barriers.

9. Hong Kong Planning Standards and Guidelines. In: Chapter 8 Internal Transport Facilities.

10. C. M. software.

11. I. S. U. C. f. N. Evaluation. "Sound." Iowa State University Center for Nondestructive Evaluation.

12. Yoshida S (2024) Propagation of Acoustic Waves in Solids pp. 87–121.

13. Redondo J, Solana RD, Picó R (2023) Increasing the Insertion Loss of Sonic Crystal Noise Barriers with Helmholtz Resonators. Applied Sciences 13(6): 3662.